Mechanics & Industry **19**, 504 (2018)

https://doi.org/10.1051/meca/2018029

Mechanics & Industry

Available online at:
www.mechanics-industry.org

Regular Article

Modeling and numerical study of H_2/N_2 jet flame in vitiated co-flow using Eulerian PDF transport approach

Ahmed Amine Larbi[1,2,*], Abdelhamid Bounif[1], and Mohamed Bouzit[3]

[1] Faculté du Génie Mécanique, Université des Sciences et de la Technologie d'Oran Mohamed Boudiaf, BP. 1505 Elmenaouer, Oran 31000, Algeria
[2] Unité de Recherche en Energies renouvelables en Milieu Saharien, URERMS, Centre de Développement des Energies Renouvelables, CDER, 01000 Adrar, Alegria
[3] Laboratoire des Sciences et Ingénierie Maritime (LSIM), Faculté du Génie Mécanique, Université des Sciences et de la Technologie d'Oran Mohamed Boudiaf, BP. 1505 Elmenaouer, Oran 31000, Algeria

Received: 20 December 2017 / Accepted: 30 May 2018

Abstract. The multi-environment Eulerian approach (MEPDF) is the eulerian method to solve the PDF transport equations; it is considered a product of the delta function. Its advantages are the prediction of extinction and ignition of the flame, also the kinetic control of the species as CO and NOX. Even though the MEPDF approach has been improved in recent years, most improvements have been achieved with parametric study in order to investigate the impact of the model accuracy. The main objective of this work is to improve further the model accuracy, the prediction of the lift off height by a parametric study of the mixing constant and Schmidt number and to understand its impact in flame stabilization. The numerical investigation of H_2/N_2 jet flame in vitiated co-flow is presented using MEPDF approach. The study was applied with K-epsilon modified model of turbulence. The chosen mixture model is the IEM (Interaction by Exchange with the Mean). The number of environment in the multi-environment Eulerian approach MEPDF is (2.0). The model was solved in this work by the commercial CFD code, ANSYS fluent and the chemical reaction mechanism injected is GRI mech 2.1. The results are validated with experimental data and discussed.

Keywords: Multi-environment Eulerian approach / PDF transport / mixing constant / Schmidt number / K-epsilon modified

1 Introduction

Industrial systems involving combustion phenomena were subject to increasingly important economic constraints (i.e. cost reductions, performance improvements) than environmental constraints (reduction of NOX, CO). These considerations motivate many research related to the reduction of pollutant emissions. So understanding, modeling and simulation not only allow for the development of new forecasting technique but also help to reduce pollutant emissions. The probability density function [1] (PDFT) is the chosen model in our study and the most suitable for the previous vision since it allows the kinetic control of the species as CO and NOX. Also, all terms characterized at a point are defined as the average chemical reaction rate. In the last decade, Haworth [2] has attracted much attention by developing the probability density function in turbulent reactive flows. The literature on hybrid approach RANS-PDFT shows two methods to solve the equation of the PDFT: Lagrangian Monte-Carlo PDF method (LPDF) and multi-environment Eulerian PDF method (MEPDF).

Lot of research on LPDF in a turbulent diffusion flame method has been done [3–12]. Several studies by application of another flame [13,14] have presented this method by applying different mixing models: modified curl, interaction by exchange with the mean (IEM) and Euclidean minimum spanning tree (EMST) to contemplate the effect of the model and to make a comparative analysis.

Few publications to solve the equation of the PDFT have appeared in recent years documenting the MEPDF. Fox et al. [15] proposed the hypothesis to clarify the presumed shape multi-environment Eulerian method (MEPDF) in turbulent reaction flow. Tang et al. [16] performed a numerical investigation with direct quadrature method of moments (DQMOM) for tested finite-rate chemistry by modeling a series of bluff-body stabilized flames and showed that the eulerian model accurately takes

* e-mail: aminelarbi@hotmail.fr

the trends exhibited among these flames. Akroyd et al. [17] introduced a new DQMoM-IEM source term for study of sensitivity and the discussion of a problem of boundedness and singularity. Yadav et al. [18] used this method of multi-environment Eulerian PDF in two turbulent lifted flames of H_2/N_2 and CH_4/air injected in vitiated coflow for numerical investigation introduced between different values of mixing constant and they found a good adequacy with experimental data. Another study by Yadav et al. [19] uses the same approach with the non-gray radiation modeling using the weighted sum of gray gases method demonstrating the promptness of a steady flame for lower estimations ($C_{\text{phi}} = 2$). On the other hand, LPDF approach found that an estimation of ($C_{\text{phi}} = 2$) prompts global extinction, the estimation of ($C_{\text{phi}} = 3$) prompts most precise outcomes. Dongre et al. [20] studied two different burners imitating moderate and intense low Oxygen Dilution MILD by multi environment PDF and showed that the difference in the predictions for Reynolds (Re) number is expanded and that is principally because of the errors in the turbulence model and wrong reaction of the micro-mixing term. Mobus et al. [21] used a flame of hydrogen for a comparative study between Lagrangian and Eulerian methods, insufficiently results owing to the use of chemical mechanism of seven elements. Two other comparative studies of both methods, the first by Jaishree et al. [22] uses the same comparison and demonstrated that the lagrangian model is much more accurate than the eulerian model. The second by Larbi et al. [23] but with an opposite demonstration, it shows that the eulerian model is much more accurate than the lagrangian model, every study has these reasons.

In this paper, the approach of hybrid RANS-MEPDF is presented. Accordingly, the method Eulerian is otherwise called multi-environment Eulerian PDF (MEPDF) or just Eulerian PDF which is determined and developed by Fox [24] in a reactive turbulent flow. Even though the MEPDF approach has been improved in recent years, most improvements have been achieved with parametric study in order to investigate the impact of the model accuracy. Nonetheless, it is possible to further improve the model accuracy, the prediction of the lift off height, the influence of mixing constant and Schmidt number; the identification of turbulent flame. With this goal, this work seeks.

2 Theoretical formulation of multi-environment Eulerian PDF transports method (MEPDF)

The generalized equation for transported PDF in a turbulent reactive flow can be written as [1]

$$\frac{\partial}{\partial t}(\rho p) + \frac{\partial}{\partial x_i}(\rho u_i p) + \frac{\partial}{\partial \psi_k}(\rho S_k p) = \frac{\partial}{\partial x_i}[\rho \langle u_i'' | \psi \rangle P] + \frac{\partial}{\partial \psi_k}\left[\rho \langle \frac{1}{\rho}\frac{\rho j_{i,k}}{\partial x_i} | \psi \rangle \mathrm{P}\right], \quad (1)$$

where P is the probability, ρ the density, u_i is the velocity, S_k is the net reaction rate and ψ is the composition space vector.

In equation (1), there is not any problems of closing in left hand, this gives the advantage and principal strength of the PDFT equation that the reaction term closed [25] and required no modeling. The first term of the equation in right hand is the turbulent scalar flux, modeled by gradient–diffusion (2).

$$-\frac{\partial}{\partial x_i}[\rho u_i'' | \psi p] = \frac{\partial}{\partial x_i}\left(\frac{\rho \mu_t}{Sc_t}\frac{\partial p}{\partial x_i}\right), \quad (2)$$

where μ_t is the turbulent viscosity, Sc_t is the Schmidt number.

Two methods of solution for closing the second term of right hand in PDF transport equation (1), LPDF and MEPDF method. In our study, we have chosen the second method of eulerian because accurate transformation of the chemical source and economical in terms of computational time or effort.

$$p(\psi;\ x\ , t) = \sum_{n=1}^{N_e} p_n(\ x\ , t) \prod_{k=1}^{N_s} \delta[\psi_K - \langle \phi_K \rangle_n(\ x\ , t)]. \quad (3)$$

Multi-environment Eulerian has been defined in an associated probability between the composition space and the physical space. The composition space is defined by a smaller number of interactive environments by the coexisting in physical space.

$$\frac{\partial \rho p_n}{\partial t} + \frac{\partial}{\partial x_i}(\rho u_i p_n) = \nabla(\rho \Gamma \nabla p_n), \quad (4)$$

$$\frac{\partial \rho s_{k,n}}{\partial t} + \frac{\partial}{\partial x_i}(\rho u_i s_{k,n}) = \nabla(\rho \Gamma \nabla s_{k,n}) + \rho(M_{k,n} + S_{k,n} + C_{k,n}). \quad (5)$$

Since micro-mixing is modeled by IEM, the turbulent scalar modeled by diffusion gradient in the transport equation for a single point multi dimensional joint composition PDF, MEPDF was derived from this equation with these terms closed in equation (3), the only problem is that we have two terms unknown.

$$S_{k,n} = p_n S(\langle \phi_K \rangle_n)_k, \quad (6)$$

$$M_{k,n} = \frac{C_\phi}{\tau}(\langle \phi_K \rangle_n - \psi_K), \quad (7)$$

where C_φ is the mixing constant, φ_K is the mean composition vector.

Marchisio and Fox [26] used as an alternative the DQMOM model (direct quadrature method of moments) to solve this problem for success. For their alternative to resolve the unknown terms, p_n and $<\phi_k>_n$. in equation (3) by using the DQMOM approach, the resulting equations for multi environment are presented in equation (4) and equation (5), where $S_{k,n}$ represents the reaction, $M_{k,n}$

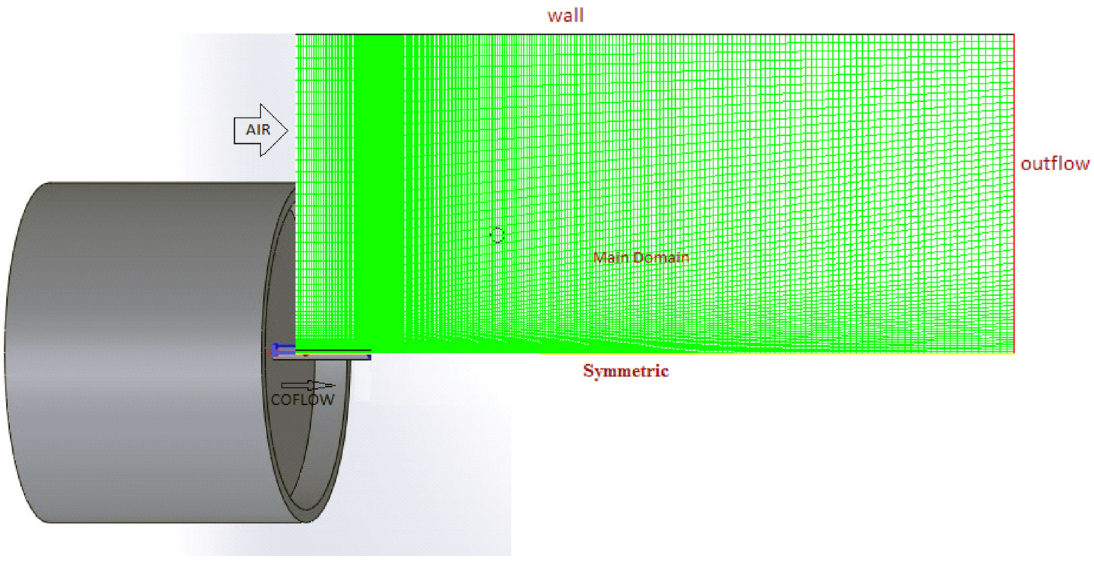

Fig. 1. Burner schematic [3] and computational domain for the simulated lifted flame of hydrogen.

represents the mixing and $C_{k,n}$ represents the correction terms

$$\sum_{n=1}^{N_e}\phi_{K_n}^{m_k-1}C_{k,n}=\sum_{n=1}^{N_e}(m_k-1)\left\langle\phi_K\right\rangle_n^{m_k-2}p_nc_{k,n}. \quad (8)$$

2.1 RANS approach turbulence model

The turbulence RANS model applied is the standard k-ε, it has been proposed by Launder and Splanding [27], which solve two transport equations to determine the turbulent length and the time scalar. The k-ε model is a first-order model based on the concept of turbulent viscosity introduced by Boussinesq.

$$\frac{\partial}{\partial t}(\rho k)+\frac{\partial}{\partial x_i}(\rho k u_i)=\frac{\partial}{\partial x_j}\left[\left(\mu+\frac{\mu_t}{\sigma_k}\right)\frac{\partial k}{\partial x_j}\right]+G_k +G_b-\rho\varepsilon-Y_M+S_k, \quad (9)$$

$$\frac{\partial}{\partial t}(\rho\varepsilon)+\frac{\partial}{\partial x_i}(\rho\varepsilon u_i)=\frac{\partial}{\partial x_j}\left[\left(\mu+\frac{\mu_t}{\sigma_\varepsilon}\right)\frac{\partial\varepsilon}{\partial x_j}\right] +G_{1\varepsilon}\frac{\varepsilon}{k}(G_k+G_{3\varepsilon}G_b)-C_{2\varepsilon}\rho\frac{\varepsilon^2}{k}+S_k. \quad (10)$$

This model is based on transport equations for the turbulent kinetic k energy that is derived from an exact equation, and its dissipation rate ε obtained from a physical reasoning. The turbulent kinetic energy k and its dissipation rate ε are obtained respectively from the two equations (9) and (10)

$$\mu_t=\rho C_\mu\frac{k^2}{\varepsilon}. \quad (11)$$

The term G_k represents the TKE of the mean velocity gradients. G_b is the generation of turbulence due to buoyancy. There are five constants in k-ε turbulence model, the turbulent Schmidt number (TSN) σ_k and σ_ε in the k. For ε we have $C\varepsilon_1$ (production of dissipation), $C\varepsilon_2$ (dissipation of dissipation) and C_μ in the expression for the apparent turbulent viscosity in equation (11).

Table 1. Base-case conditions for the vitiated coflow burner.

	Jet	Coflow
Re	23.600	18.600
D(mm)	4.57	210
V(m/s)	107	3.5
T(k)	305	1045
X_{H_2}	0.2537	0.0005
X_{O_2}	0.0021	0.15
X_{N_2}	0.7427	0.75
X_{H_2O}	0.0015	0.099

3 Flame of vitiated coflow

The flames of hydrogen considered in the current work have already been studied experimentally by Cabra et al. [3]. The burner consists of a horizontal tube with an internal diameter (D) of 4.57 mm and an outside diameter of 6.35 mm, centered in a cross-section with an internal diameter of 210 mm (Fig. 1). The computational domain contains fuel jet, pilot stream, surrounding air and main domain with 15520 cells (fine-1). Concerning the study of grid independence test, we proposed two other non-uniform distinct grids: base with 18220 cells and fine-2 with 35320 cells. Base-case conditions for the vitiated coflow burner are given by Table 1.

The configuration of the geometry is axisymmetric with a quadrilateral mesh shape. The ANSYS-Fluent 15.0 CFD

Table 2. Base-case conditions for the turbulence model and the mixing constant.

Cmu	C1	C2	TKE	TDR	TSN	$C\varphi$
0.09	1.55	1.92	1	1.22	0.7	1.8

software is used to simulate the burner in a Cartesian coordinate-system. A refining of the zones near the exit of the burner has been envisaged to take into account the large variations taking place in these zones, in particular velocity gradients. Table 2 shows the initial conditions, the definition of the geometry and the generation of the mesh were carried out using ANSYS-Workbench15.0.

The turbulence is modeled by modified standard k-ε model, that we played on some influential parameters in the MEPDF method like the number of schmidt so that the model of turbulence (k-ε) will be modified and gives good results with the MEPDF method. The optimal value of TSN is (0.9), and the other values are presented in Table 2. A second-order upwind scheme is used in all equations conservation for modeling the convective flux. The MEPDF is used with the value of (1.8) in the mixing constant and combustion chemistry using in situ adaptive tabulation method ISAT [28]. The chemical reaction mechanism adopted is GRI-Mech2.1. Environment number equal two in the first approach ($N_e = 2$).

4 Results and discussion

The study of MEPDF approach using turbulent lifted flame of H_2/N_2 in hot vitiated coflow is presented in the current section.

4.1 GRID-independent study

Figure 2 shows radial profiles of density and velocity at axial location of $X/D = 14$ for MEPDF method. Each plot shows three profiles for meshes 1, 2 and 3. Meshes 2 and 3 give very close results and either may be used to produce a grid independent solution. Mesh-1 shows only slight departures from meshes 2 and 3, especially for velocity. Figure 3 shows axial profiles of temperature and mixture fraction from three different meshes. We can see that the predictions of temperature using three meshes are in good agreement with each other while the peak temperatures obtained with four meshes (mesh-1, mesh-2, and mesh-3) are 1513 k, 1510 k and 1508 k. The peak temperature of experimental data is 1498 k which helps us to confirm that the meshes are in good agreement. We can see in the predictions using the different grids that differences between coarsest and finest mesh are less than 3%. In mixture fraction profile, we can see the predictions of mesh-1 showing only slight departures from mesh-3, but mesh-2 gives very close results with mesh-3. Therefore, from Figures 2 and 3, mesh-2 and mesh-3 give very close results and either may be used to produce a grid independent solution. However, mesh-2 is selected here and is used in all further calculations.

4.2 Flame of hydrogen in a hot vitiated coflow

Figure 4 shows the contours of temperature, mixture fraction and species mass fractions inside computational domain along centerline for MEPDF approach. For the temperature contour, we can see an output of the reactants at the beginning of the nozzle. These reactants being separated, the zone of premixing is located immediately after, where the fuel and the oxidizer are in a mixture. This mixture is due to the concentration gradient. We have a kinetically controlled environment that is pre-lit, but does not ignite because of chemical delays up to the point of $X/D = 5$ of the jet exit. Afterwards, we notice an increase in temperature. This increase is due to two phenomena, the first is due to the hot coflow, the second is because of the start of the reaction chain, this increase is noticed by the degradation of the hydrogen fraction and the production of the fraction of OH, up to the point of $X/D = 30$. Thereafter, the decrease of temperature until reached the co-flow temperature. The detailed explanations are given in the next section.

Figure 5 shows the axial profiles of temperature, mixture fraction and species mass fractions along the centerline compared with the experimental data [7]. For profile of temperature, we can see that the increase of temperature at the centerline starts up from the jet exit until ($X/D = 10$), this rise is primarily due to the mixing and preheating. This increase continues until ($X/D = 30$) which is due to the chemistry reactions, after the start of the reactions we have the diffusion of height temperature until the maximum temperature reached, thereafter where ($X/D > 30$) the decrease of temperature until reached the co-flow temperature. The current predictions of MEPDF in profile of temperature are in good agreement with the experimental values in all locations. The height temperature of the flattened peak between experiment and calculation does not exceed 12 k.

For mixture fraction profile, the current predictions obtained are compatible with the experimental results. After ($X/D = 20$), under-prediction is observed for the calculated results against the experiment data until ($X/D = 35$) which is due to the turbulence models (the turbulent mixtures and the turbulent viscosity) [18]. The exact forecast of OH is of prime significance and essential criteria to judge the MEPDF model exactness and capability. In OH profile, we can see from the jet exit no production in mass fraction of OH until ($x/d = 10$) and thereafter the startup of OH production until ($x/d = 30$). Even after the end in production of OH, the consumption continues for produce H_2O, since the latter is produced by the oxidation of OH radicals. The difference between the peak of computed values and the experimental value in OH mass fraction is less than 2%. The predictions of MEPDF are in good adequacy with the experimental values and also it's better than the computed results of Yadav et al. [18].

Moreover, it is observed in H_2O mass fraction curve, a very good agreement between the calculated values of MEPDF and the experimental values. Similarly in H_2 profile, we can see that the predictions of MEPDF are in good agreement with the experimental values.

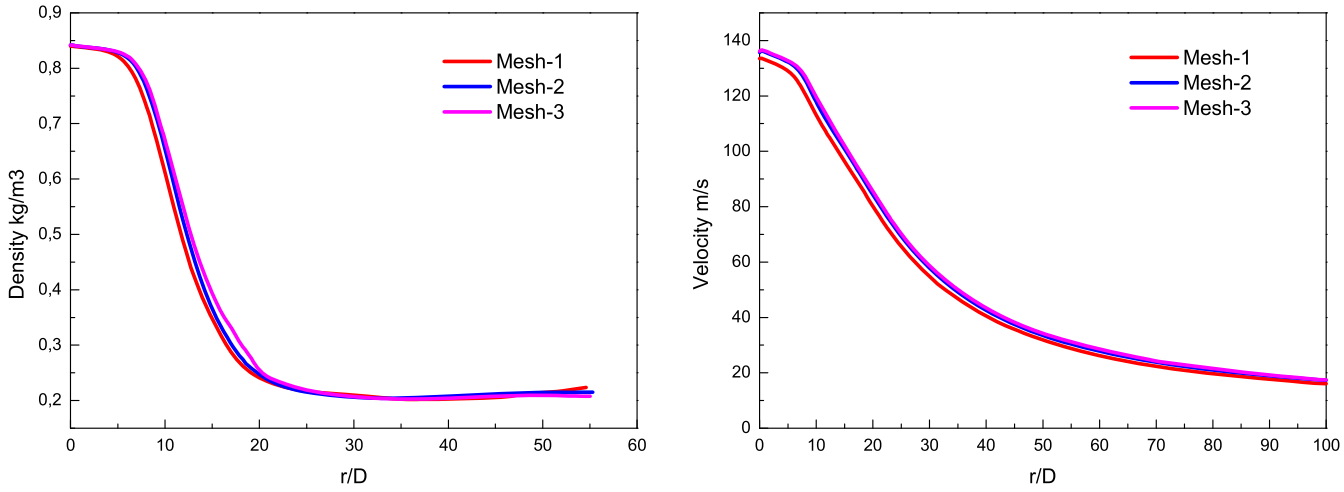

Fig. 2. Axial profiles of density and velocity along centerline for approach of MEPDF.

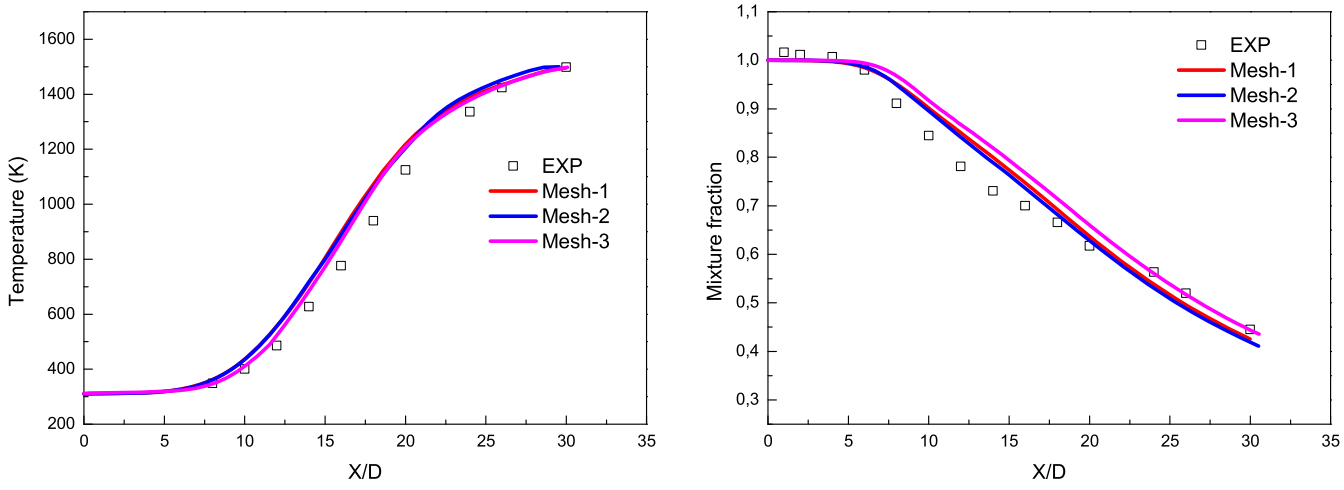

Fig. 3. Axial profiles of temperature and mixture fraction along centerline for approach of MEPDF.

In O_2 profile, we notice that the prediction of MEPDF is in good agreement with the experimental data. The peak of O_2 is in the point of $(X/D = 13)$, showing the upstream penetration which is increased with the lift-off height. The peak also shows the consumption of O_2 by the flame. The difference between the peak of MEPDF values and the experimental value is due to the sensitivity of the predicted rates mixing to the turbulence model [3].

Figure 6 presents the radial profiles of temperature, mixture fraction and species mass fractions at axial location of $X/D = 14$ and $X/D = 26$ for MEPDF approach with the experimental values [7]. We can see for the two temperatures and mixture fraction profiles that the current prediction of the MEPDF approach is in very good agreement with the experimental data for each axial location. In the OH curve, we observed in each axial location, the found results are in excellent agreement with the experimental data. The model prediction for $X/D = 14$ shows a lower value of sharp peak than experimental of OH, which means a shorter prediction of flame (lift-off height). In H_2 profile, we can see for the two axial locations, a good agreement with the experiment values. In the second axial location of H_2 profile for $X/D = 26$, we have an anomalous low value of H_2 in MEPDF approach at centerline as a result of very high consumption of H_2. This consumption is due to the early starting of reaction.

4.3 The influence of mixing constant and the Schmidt number

Cao et al. [12] performed a sensitivity study on constant mixing model in a turbulent flame of lifted vitiated coflow by LPDF method. Yadav et al. [18] studied the MEPDF method with IEM of mixing model and found a reasonable prediction with constant of $(C\varphi = 2)$, as for the locations of the peak, they are slightly affected by the change. Concerning the prediction of OH, a significant difference

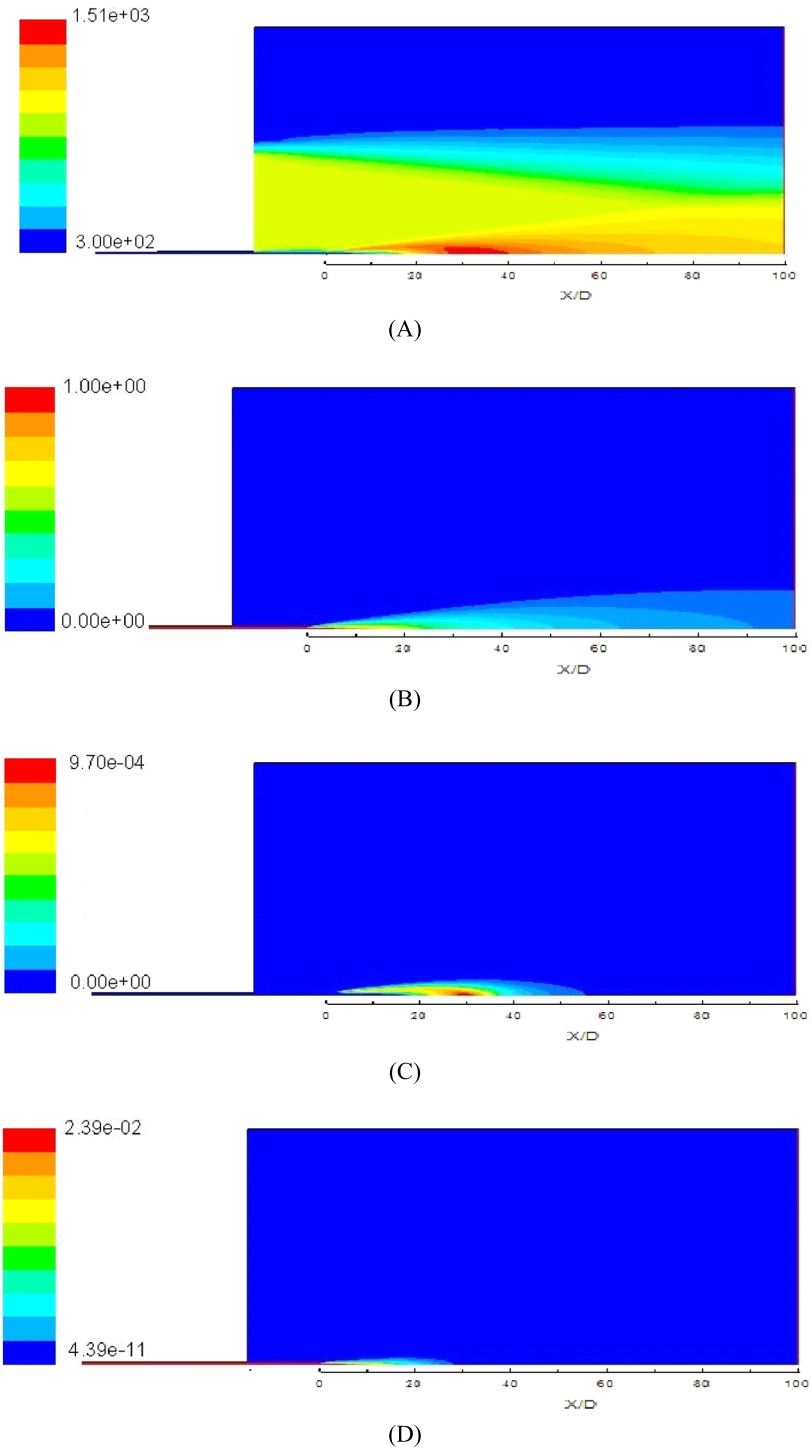

Fig. 4. Temperature (A), mixture fraction (B), OH mass fraction (C), and H_2 mass fraction (D), contours inside computational domain along centerline for MEPDF approach.

is obtained between different $C\varphi$ values, the maximum OH value increases by 30% when $C\varphi$ changes from 1.5 to 4.0. In addition, the OH profile with a $C\varphi = 3$ value is considered as the most accurate. Yadav et al. [18] found a good prevision for lift-off height with a value of 1.5, even if we still reduce it, but with a slight difference in the temperature profile. In our present study it was found that the results of this flame and the application of the MEPDF approach are influenced by two parameters; the constant of mixing and the number of Schmidt. With respect to the first parameter, with a constant of 1.8, a good result can be obtained at both the level of the temperature profile and the level of the OH prediction. Lift-off height will be discussed.

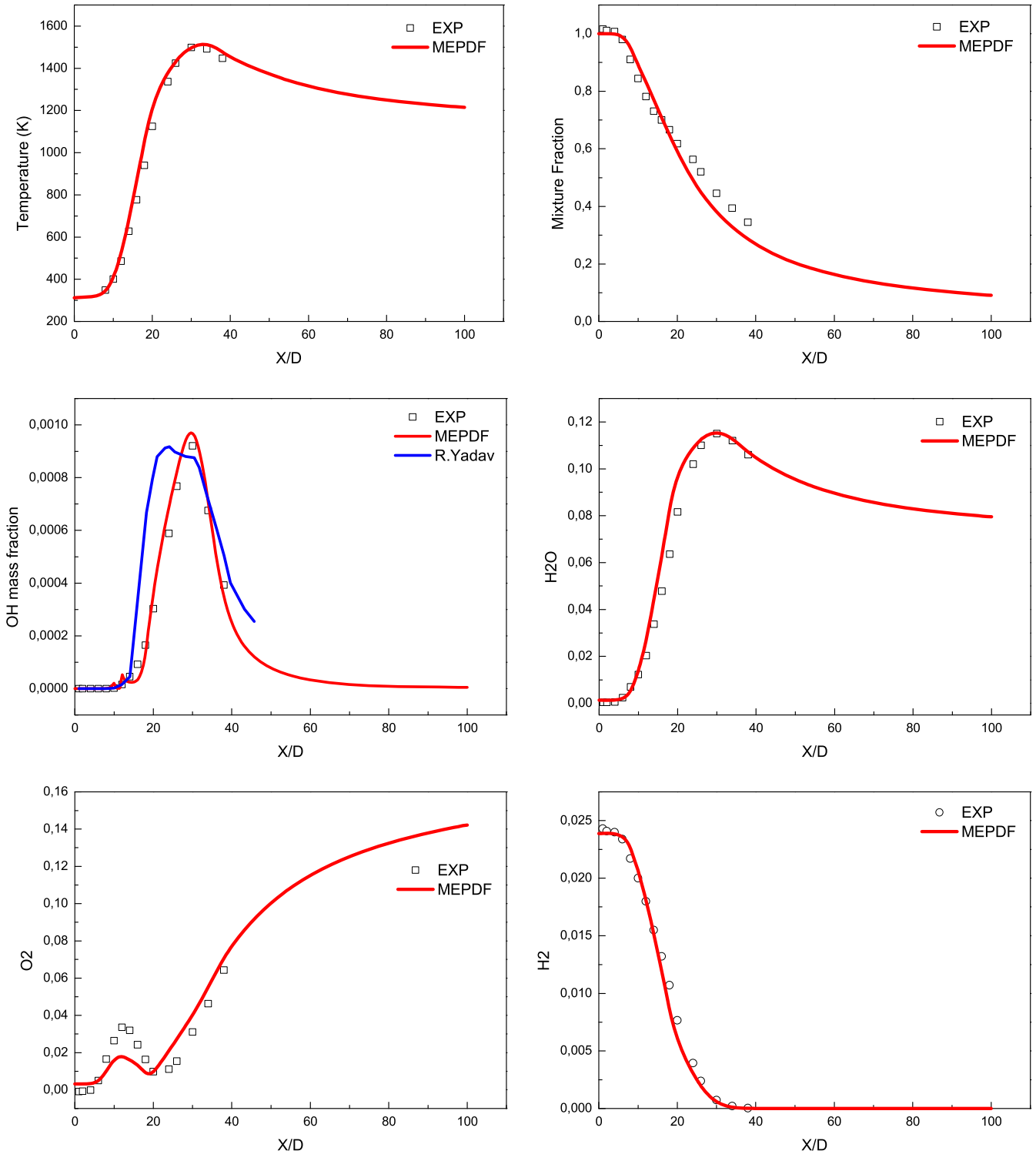

Fig. 5. Axial profiles of temperature and species mass fractions along centerline for MEPDF approach.

4.3.1 The influence of mixing constant

We studied the sensitivity of the mixing constant on the MEPDF approach and showed its influence on lift-off height and results. Five values of $C\varphi$ are used between 1.5 and 3.0, with a Schmidt number of 0.7. Figure 7 shows the axial profiles of temperature and species mass fractions along centerline with different $C\varphi$. The temperature profile shows a difference in temperatures and their location, each mixing constant has a different peak against the others. Between the constants of 1.5 and 3.0, we have an interval of maximum temperatures of (1507 K

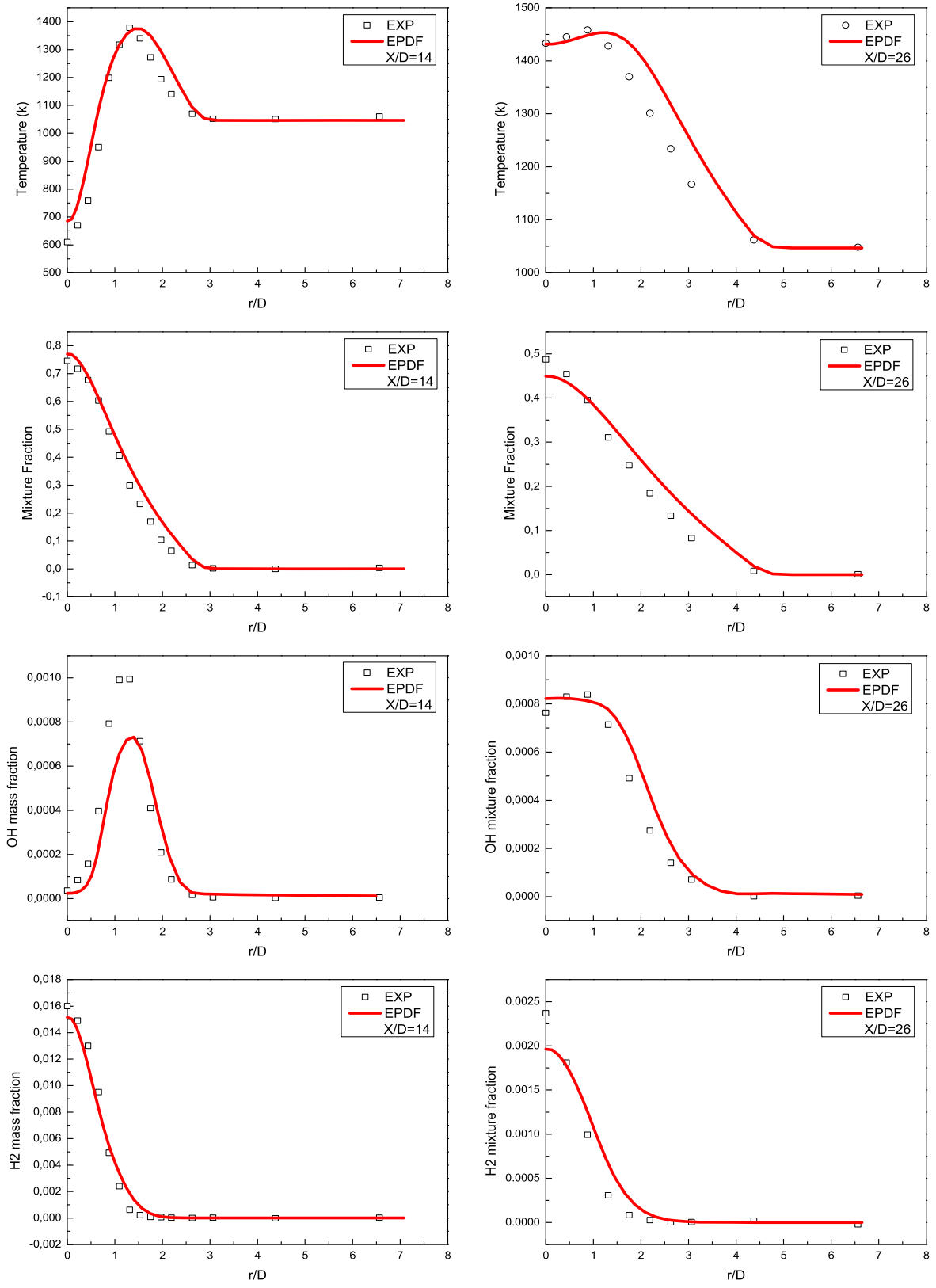

Fig. 6. Radial profiles of temperature, mixture fraction and species mass fractions at locations of $X/D = 14$, 26.

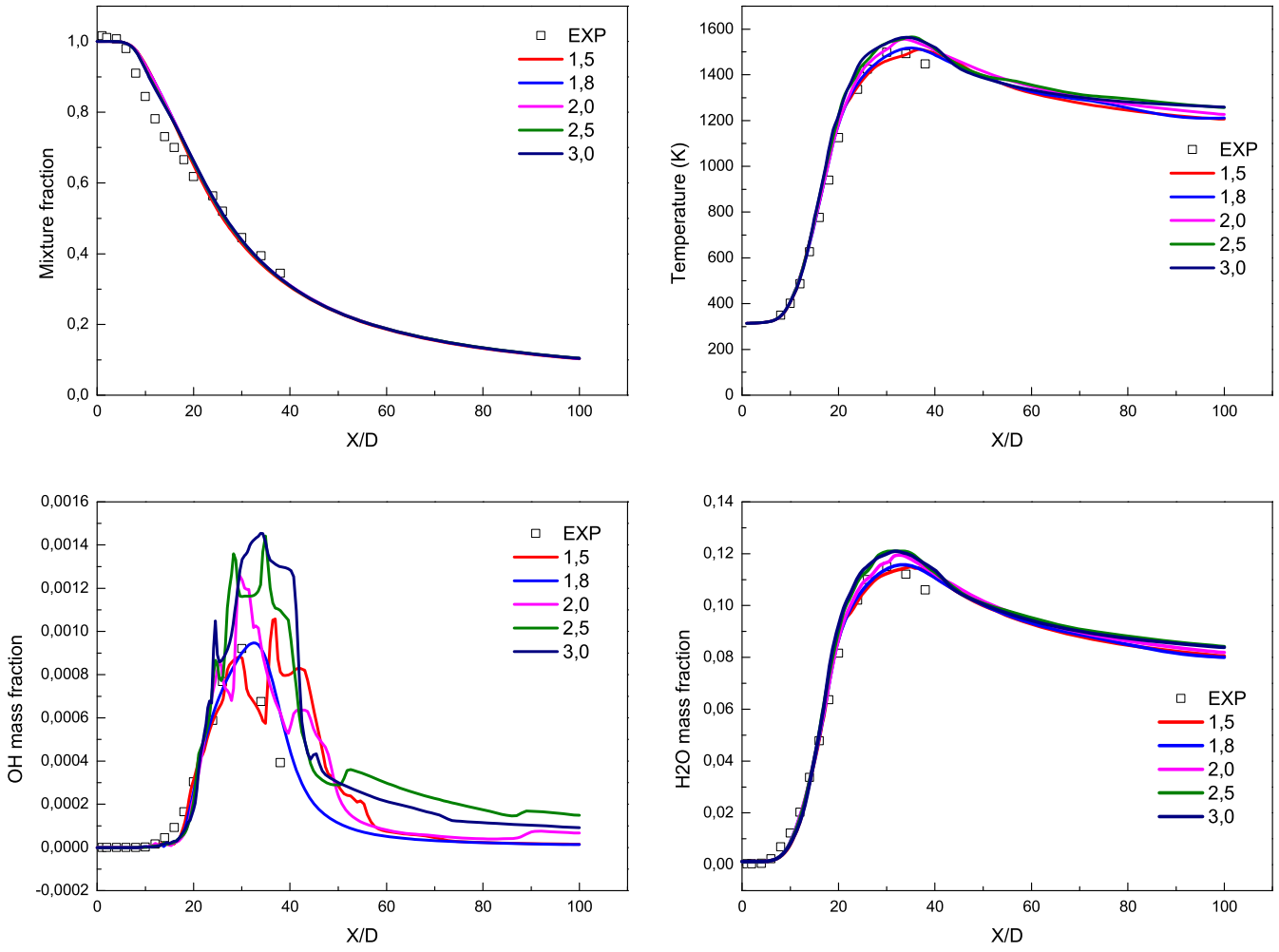

Fig. 7. Axial profiles of temperature and species mass fractions along centerline with different $C\varphi$.

and 1559 K) with a displacement of $(32 < X/D < 35)$. In addition, we have found that two mixing constants ($C_\phi = 1.5, 1.8$) give good agreement with the experimental data. The similar behavior is observed for H_2O curve. The profile of the mixture fraction gives similar results for all mixing constants. The results are in good agreement with the experimental data, with a slight difference in the range of $(5 < X/D < 15)$ for all mixing constant in the mixture fraction curve, this slight difference is due to the turbulence model and will be eliminated or corrected in the influence step of Schmidt number .The only exception is in the OH curve, a nearly random behavior is observed for all the mixing constants, except for the mixing constant of 1.8, it is more precise and in good agreement with the experiment data. In the next step, we will try to improve the prediction of OH by other parameters.

4.3.2 The influence of Schmidt number

We investigated the sensitivity of the Schmidt number on the MEPDF approach and showed its influence on the results. Four values of Schmidt number = 0.7, 0.9, 1.2 and 1.4 are used, with a mixing constant of 0, 8. Figure 8 shows the axial profiles of temperature and species mass fractions along centerline with different Schmidt numbers. The temperature profile shows a difference in temperature and their location, each Schmidt number has a different peak against the others. Between the Schmidt numbers of 0.7 and 1.4, we have an interval of maximum temperatures of (1501 k and 1517 k) with a displacement of $(30 < X/D < 38)$. In addition, we have found that Schmidt number of 0.7 gives good agreement with the experimental data. The profile of the mixture fraction gives similar results for all Schmidt numbers. The results are in good agreement with the experimental data. A similar behavior is observed for the H_2O mass fraction curve. In the OH curve, the first finding is that the randomness observed in the old OH curve is eliminated for all the variables of the Schmidt number. The second observation is that for the three Schmidt values (0.7, 0.9, and 1.2), we have almost good results. The last Schmidt number (1.4) has inaccurate results and doesn't satisfy the experimental data. Finally, we can have a good agreement for results with a Schmidt number of 0.7 and constant mixing of 1.8 compared to the experimental data, such as the temperature results, OH and any other fraction, even for lift-off height.

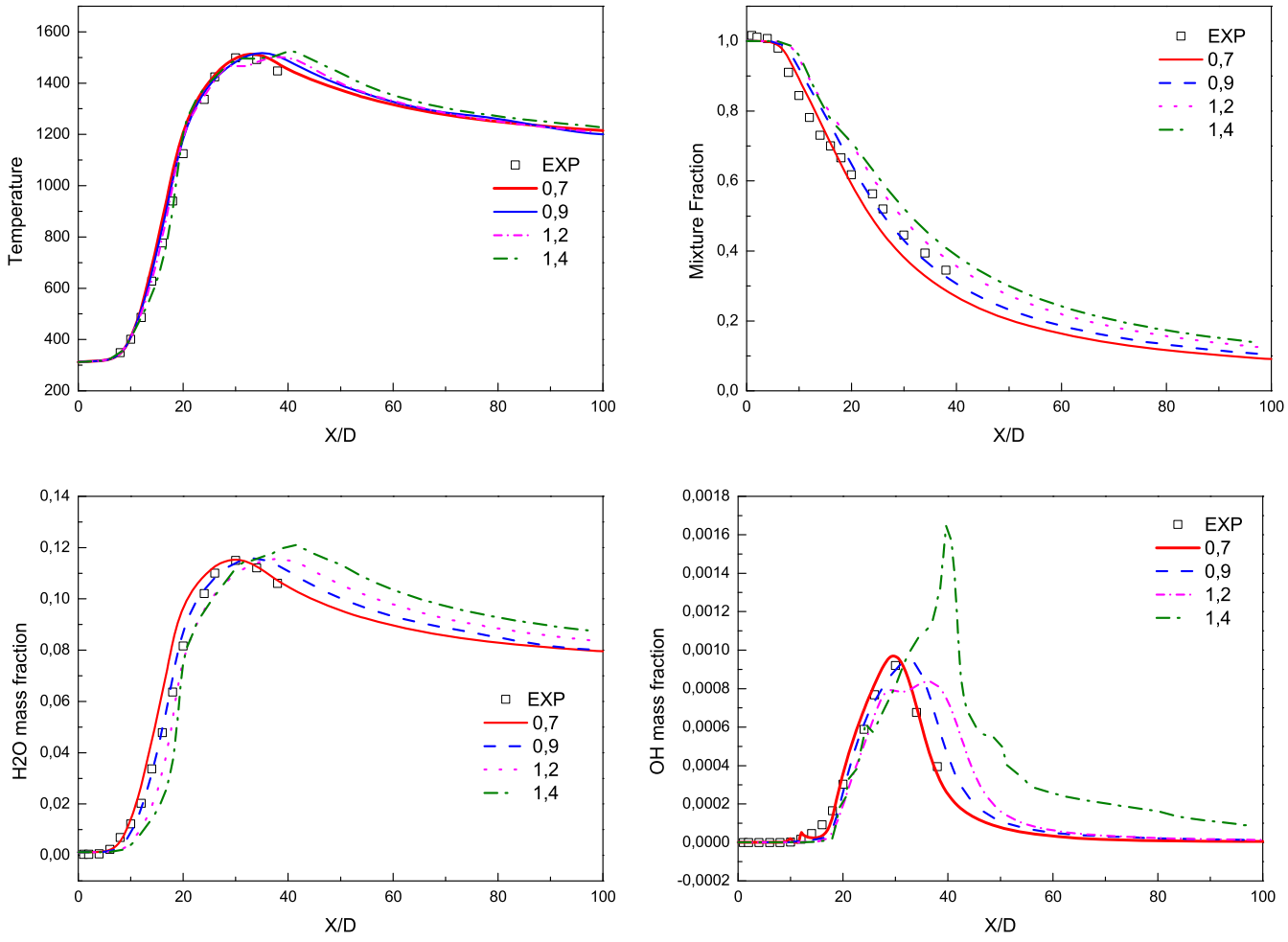

Fig. 8. Axial profiles of temperature and species mass fractions along centerline with different Schmidt number.

5 Conclusions

In this paper, we applied the Eulerian (MEPDF) approach to study the turbulent diffusion flame of hydrogen (H_2). The selected turbulence model is k-ε modified and IEM mixing model. Based on the results, it can be concluded that the MEPDF approach is very promising. It is very important to identify turbulent flame and crucial to predict the local extinction, reignition. The height temperature of the flattened peak between experiment and calculation does not exceed 12 k. The current predictions of temperature profile and all mass fractions are compatible with the experimental results. The good prevision of OH in the current study is one of prime essential criteria to judge the MEPDF model exactness and capability. The sensitivity study is presented with the mixing constant and Schmidt number in the MEPDF approach to show the influence of different $C\varphi$ values and Schmidt number on lift-off height and results. We found good results for all the constant mixing, except the OH curve, a nearly random behavior is observed unless the mixing constant was 1.8, which is the most precise and in good agreement with the experiment data. Finally, we can have a good agreement for results with a Schmidt number of 0.7 and constant mixing of 1.8 compared to the experimental data, such as the temperature results, OH and any other fraction, even for lift-off height. In conclusion, it is evident that this study has shown the value of the MEPDF model, the ease of having good results and with minimal cost. On the basis of the promising findings presented in this paper, work on the remaining issues is continuing and will be presented in the future papers.

References

[1] S.B. Pope, PDF methods for turbulent reactive flows, Prog. Energy Combust. Sci. 11 (1985) 119–193
[2] D.C. Haworth, Progress in probability density function methods for turbulent reacting flows, Prog. Energy Combust. Sci. 36 (2010) 168–259
[3] R. Cabra, J.Y. Chen, R.W. Dibble, Y. Hamano, A.N. Karpetis, R.S. Barlow, Simultaneous Raman-Reyleigh-LIF measurements and numerical modeling results of a lifted H2/N2 turbulent jet flame in a vitiated coflow, NASA Rep. 212081 (2002) 1881–1888
[4] V. Saxena, S.B. Pope, PDF calculations of major and minor species in a turbulent piloted jet flame, Symp. Combust. 27 (1998) 1081–1086

[5] M. Muradoglu, S.B. Pope, D.A. Caughey, The hybrid method for the pdf equations of turbulent reactive flows: consistency conditions and correction algorithms, J. Comp. Phys. 172 (2001) 841–878
[6] M. Muradoglu, K. Liu, S.B. Pope, PDF modeling of a bluff-body stabilized turbulent flame, Combust. Flame 132 (2003) 115–137
[7] R. Cabra, J.Y. Chen, R.W. Dibble, A.N. Karpetis, R.S. Barlow, Lifted methane-air jet flames in a vitiated coflow, Combust. Flame 143 (2005) 491–506
[8] R. Cao, S.B. Pope, Numerical integration of stochastic differential equations: weak second-order mid-point scheme for application in the composition PDF method, J. Comput. Phys. 185 (2003) 194–212
[9] A.R. Masri, R.R. Cao, S.B. Pope, G.M. Goldin, PDF calculations of turbulent lifted flames of H2/N2 fuel issuing into a vitiated co-flow. Combust. Theory Model. 8 (2004) 1–22
[10] K. Liu, S.B. Pope, D.A. Caughey, Calculations of bluff-body stabilized flames using a joint probability density function model with detailed chemistry, Combust. Flame 141 (2005) 89–117
[11] R.L. Gordon, A.R. Masri, S.B. Pope, G.M. Goldin, Transport budgets in turbulent lifted flames of methane autoigniting in a vitiated co-flow, Combust. Flame 151 (2007) 495–511
[12] R.R. Cao, S.B. Pope, A.R. Masri, Turbulent lifted flames in a vitiated coflow investigated using joint PDF calculations, Combust. Flame 142 (2005) 438–453
[13] R.R. Cao, H. Wang, S.B. Pope, The effect of mixing models in PDF calculations of piloted jet flames, Proc. Combust. Inst. 31 (2007) 1543–1550
[14] M. Senouci, A. Bounif, M. Abidat, N.M. Belkaid, C. Mansour, I. Gokalp, Transported-PDF (IEM, EMST) micromixing models in a hydrogen-air nonpremixed turbulent flame, Acta Mech. 224 (2013) 3111–3124
[15] R.O. Fox, A. Varma, Computational models for turbulent reacting flows, Cambridge Univ. Press (2003)
[16] Q. Tang, W. Zhao, M. Bockelie, R.O. Fox, Multi-environment probability density function method for modelling turbulent combustion using realistic chemical kinetics, Combust. Theory Model. 11 (2007) 889–907
[17] J. Akroyd, A.J. Smith, L.R. Mcglashan, M. Kraft, Numerical investigation of DQMoM-IEM as a turbulent reaction closure, Chem. Eng. Sci. 65 (2010) 1915–1924
[18] R. Yadav, A. Kushari, A. De, Modeling of turbulent lifted flames in vitiated co-flow using multi environment Eulerian PDF transport approach, Heat Mass Transf. 77 (2014) 230–246
[19] R. Yadav, A. Kushari, V. Eswaran, A.K. Verma, A numerical investigation of the Eulerian PDF transport approach for modeling of turbulent non-premixed pilot stabilized flames, Combust. Flame 160 (2013) 618–634
[20] A. Dongre, A. De, R. Yadav, Numerical investigation of MILD combustion using multi-environment Eulerian probability density function modeling, Inter. J. Spray Combust. Dyn. 6 (2014) 357–386
[21] H. Möbus, P. Gerlinger, D. Brüggemann, Comparison of Eulerian and Lagrangian Monte Carlo PDF methods for turbulent diffusion flames, Combust. Flame 124 (2001) 519–534
[22] J. Jaishree, D.C. Haworth, Comparisons of Lagrangian and Eulerian PDF methods in simulations of non- premixed turbulent jet flames with chemistry interactions, Combust. Theory Model. 16 (2012) 435–463
[23] A.A. Larbi, A. Bounif, M. Bouzit, Comparisons of LPDF and MEPDF for lifted H2/N2 jet flame in a vitiated coflow, Inter. J. Heat Technol. 36 (2018) 133–140
[24] R.O. Fox, Computational models for turbulent reacting flows, Chem. Eng. 51 (2003) 215–243
[25] S.B. Pope, Lagrangian PDF methods for turbulent flows, Annu. Rev. Fluid Mech. 26 (1994) 23–63
[26] D.L. Marchisio, R.O. Fox, Solution of population balance equations using the direct quadrature method of moments, J. Aerosol Sci. 36 (2005) 43–73
[27] B.E. Launder, D.B. Spalding, The numerical computation of turbulent flows, in: Numerical Prediction of Flow, Heat Transfer, Turbulence and Combustion, Elsevier, 1983, pp. 96–116
[28] S.B. Pope, Computationally efficient implementation of combustion chemistry using in situ adaptive tabulation, Combust. Theory Model. 1 (1997) 41–63

Cite this article as: A.A. Larbi, A. Bounif, M. Bouzit, Modeling and numerical study of H_2/N_2 jet flame in vitiated co-flow using Eulerian PDF transport approach, Mechanics & Industry **19**, 504 (2018)